EPJ Web of Conferences 80, 00053 (2014)
DOI: 10.1051/epjconf/20148000053


# Electroweak chiral Lagrangians and the Higgs properties at the one-loop level

J.J. Sanz-Cillero[1,a]

[1] *Departamento de Física Teórica and Instituto de Física Teórica, IFT-UAM/CSIC Universidad Autónoma de Madrid, C/ Nicolás Cabrera 13-15, Cantoblanco, 28049 Madrid, Spain*

**Abstract.** In these proceedings we explore the use of (non-linear) electroweak chiral Lagrangians for the description of possible beyond the Standard Model (BSM) strong dynamics in the electroweak (EW) sector. Experimentally one observes an approximate EW symmetry breaking pattern $SU(2)_L \times SU(2)_R/SU(2)_{L+R}$. Quantum Chromodynamics (QCD) shows a similar chiral structure [1] and, in spite of the differences (in the EW theory $SU(2)_L \times U(1)_Y$ is gauged), it has served for years as a guide for this type of studies [2–4]. Examples of one-loop computations in the low-energy effective theory and the theory including the first vector (V) and axial-vector (A) resonances are provided, yielding, respectively, predictions for $\gamma\gamma \to Z_L Z_L, W_L^+ W_L^-$ and the oblique parameters $S$ and $T$.

## 1 Introduction: strong dynamics and chiral Lagrangians

A non-linear realization of the EW would-be Goldstone bosons (WBGBs) is considered to build the EW low-energy effective field theory (EFT), which is described by an EW chiral Lagrangian with a light Higgs (ECLh). It includes the Standard Model (SM) content: the EW Goldstones $w^a$, the EW gauge bosons $W_\mu^a$ and $B_\mu$ and a singlet Higgs $h$ (the fermion sector is not discussed here). In particular, in Sec. 2 we explain the chiral counting in the ECLh [5, 6] and provide an example of a next-to-leading order (NLO) computation: we calculate $\gamma\gamma \to W_L^+ W_L^-$, $Z_L Z_L$ within this framework up to the one-loop level [5] at energies below new possible composite resonances, $\sqrt{s} \ll \Lambda_{\rm ECLh} \sim \min\{M_R, 4\pi v\}$ (with $v = (\sqrt{2}G_F)^{-1/2}$ and $4\pi v \simeq 3$ TeV). Analogous works on $WW$–scattering can be found in Refs. [7].

However, in the case of having heavy composite resonance, the EFT stops being valid when the energy becomes of the order of their masses (expected to be of the order of $M_R \sim 4\pi v \sim 3$ TeV). One has to introduce these new degrees of freedom in our EW Lagrangian following a procedure analogous to that in QCD [8]. Likewise, under reasonable ultraviolet (UV) completion hypotheses like, e.g., the Weinberg sum-rules (WSRs) fulfilled by certain types of theories [9–13], one can make predictions on low-energy observables. In Sec. 3 we write down the relevant $SU(2)_L \times SU(2)_R$ invariant Lagrangian including the SM content and a multiplet of V and A resonances and extract one-loop limits on the resonance masses and the Higgs coupling $g_{hWW}$ [14] from the experimental values of oblique parameters $S$ and $T$ [15]. Alternative one-loop analyses can be found in Refs. [10, 16].

[a] e-mail: juanj.sanz@uam.es

I would like to thank the organizers for their work and the lively discussion during the workshop; also for their patience. This work is partially supported by the Spanish Government and ERDF funds from the European Commission [FPA2010-17747, FPA2013-44773-P, SEV-2012-0249, CSD2007-00042] and the Comunidad de Madrid [HEPHACOS S2009/ESP-1473].

## 2 Low-energy EFT: ECLh and one-loop $\gamma\gamma \to W_L^a W_L^b$ scattering

The Higgs boson does not enter in the SM at tree-level in these processes (where one also has $\mathcal{M}(\gamma\gamma \to ZZ)^{\rm tree}_{\rm SM} = 0$). Nevertheless, one can search for new physics by studying the one-loop corrections [5], which are sensitive to deviations from the SM in the Higgs boson couplings. Our analysis [5] is performed in the Landau gauge and making use of the Equivalence Theorem (Eq.Th.) [17],

$$\mathcal{M}(\gamma\gamma \to W_L^a W_L^b) \quad\simeq\quad -\mathcal{M}(\gamma\gamma \to w^a w^b)\,, \tag{1}$$

valid in the energy regime $m_W^2, m_Z^2 \ll s$. The EW gauge boson masses $m_{W,Z}$ are then neglected in our computation. Furthermore, since $m_h \sim m_{W,Z} \ll 4\pi v \simeq 3$ TeV we also neglect $m_h$ in our calculation. In summary, the applicability range in [5] is

$$m_W^2,\, m_Z^2,\, m_h^2 \quad \overset{\rm Eq.Th.}{\ll} \quad s,\, t,\, u \quad \overset{\rm EFT}{\ll} \quad \Lambda^2_{\rm ECLh}\,, \tag{2}$$

with the upper limit given by the EFT cut-off $\Lambda_{\rm ECLh}$, expected to be of the order of $4\pi v \simeq 3$ TeV or the mass of possible heavy BSM particles.

The WBGBs are described by a matrix field $U$ that takes values in the $SU(2)_L \times SU(2)_R / SU(2)_{L+R}$ coset, and transforms as $U \to LUR^\dagger$ [2, 3]. The relevant ECLh with the basic building blocks is

$$\begin{aligned} &U = u^2 = 1 + iw^a\tau^a/v + \mathcal{O}(w^2)\,,\; D_\mu U = \partial_\mu U + i\hat{W}_\mu U - iU\hat{B}_\mu\,,\; V_\mu = (D_\mu U)U^\dagger\,,\;\; u^\mu = -i\,u^\dagger D^\mu U\,u^\dagger\,,\\ &\hat{W}_{\mu\nu} = \partial_\mu \hat{W}_\nu - \partial_\nu \hat{W}_\mu + i[\hat{W}_\mu, \hat{W}_\nu], \quad \hat{B}_{\mu\nu} = \partial_\mu \hat{B}_\nu - \partial_\nu \hat{B}_\mu, \quad \hat{W}_\mu = gW^a_\mu\tau^a/2,\; \hat{B}_\mu = g'\,B_\mu\tau^3/2\,, \end{aligned} \tag{3}$$

with well-defined trasnformation properties [3, 5, 14]. Two particular parametrizations of the unitary matrix $U$ (exponential and spherical) were considered in [5], both leading to the same predictions for the physical (on-shell) observables. [1] We consider the counting $\partial_\mu$, $m_W$, $m_Z, m_h \sim \mathcal{O}(p)$, $D_\mu U$, $V_\mu \sim \mathcal{O}(p)$ and $\hat{W}_{\mu\nu}$, $\hat{B}_{\mu\nu} \sim \mathcal{O}(p^2)$ [5, 6]. We require the ECLh Lagrangian to be CP invariant, Lorentz invariant and $SU(2)_L \times U(1)_Y$ gauge invariant. Here we focus ourselves on the relevant terms for $\gamma\gamma \to w^a w^b$ at leading order (LO) –$\mathcal{O}(p^2)$– and NLO in the chiral counting –$\mathcal{O}(p^4)$– [3, 5]:

$$\begin{aligned} \mathcal{L}_2 &= -\frac{1}{2g^2}\langle\, \hat{W}_{\mu\nu}\hat{W}^{\mu\nu}\,\rangle - \frac{1}{2g'^2}\langle\, \hat{B}_{\mu\nu}\hat{B}^{\mu\nu}\,\rangle + \frac{v^2}{4}\left[1 + 2a\frac{h}{v} + b\frac{h^2}{v^2}\right]\langle\, D^\mu U^\dagger D_\mu U\,\rangle + \frac{1}{2}\partial^\mu h\,\partial_\mu h + \dots\,, \\ \mathcal{L}_4 &= a_1 {\rm Tr}(U\hat{B}_{\mu\nu}U^\dagger\hat{W}^{\mu\nu}) + ia_2{\rm Tr}(U\hat{B}_{\mu\nu}U^\dagger[V^\mu, V^\nu]) - ia_3{\rm Tr}(\hat{W}_{\mu\nu}[V^\mu, V^\nu]) - \frac{c_\gamma}{2}\frac{h}{v}e^2 A_{\mu\nu}A^{\mu\nu} \;+\; ... \end{aligned} \tag{4}$$

where $\langle X\rangle$ stands for the trace of the $2\times2$ matrix $X$, one has the photon field strength $A_{\mu\nu} = \partial_\mu A_\nu - \partial_\nu A_\mu$ and the dots stand for operators not relevant within our approximations for $\gamma\gamma$-scattering [5].

The amplitudes $\mathcal{M}(\gamma(k_1,\epsilon_1)\gamma(k_2,\epsilon_2) \to w^a(p_1)w^b(p_2))$, with $w^a w^b = zz, w^+w^-$, have the structure

$$\mathcal{M} = ie^2(\epsilon_1^\mu\epsilon_2^\nu T^{(1)}_{\mu\nu})A(s,t,u) + ie^2(\epsilon_1^\mu\epsilon_2^\nu T^{(2)}_{\mu\nu})B(s,t,u), \tag{5}$$

written in terms of the two independent Lorentz structures $T^{(1,2)}_{\mu\nu} \sim \mathcal{O}(p^2)$ involving the external momenta, which can be found in [5]. The Mandelstam variables are defined as $s = (p_1+p_2)^2$, $t = (k_1 - p_1)^2$ and $u = (k_1 - p_2)^2$ and the $\epsilon_i$'s are the polarization vectors of the external photons.

In dimensional regularization, our NLO computation of the $\mathcal{M}(\gamma\gamma \to w^a w^b)$ amplitudes can be systematically sorted out in the form [5]

$$\mathcal{M} = \mathcal{M}_{\rm LO} + \mathcal{M}_{\rm NLO} \quad\sim\quad \underbrace{\mathcal{O}(e^2)}_{\rm LO,\,tree} \quad+\quad \left(\underbrace{\mathcal{O}\left(e^2\frac{p^2}{16\pi^2v^2}\right)}_{\rm NLO,\,1-loop} \quad+\quad \underbrace{\mathcal{O}\left(e^2\frac{a_ip^2}{v^2}\right)}_{\rm NLO,\,tree}\right)\,, \tag{6}$$

[1] Other representations have been recently studied in Ref. [18].

**Table 1.** Running $\frac{da_i^r}{d\ln\mu} = -\frac{\Gamma_{a_i}}{16\pi^2}$ of the relevant ECLh parameters and their combinations appearing in the six selected observables. The third column provides the corresponding running for the Higgsless EW chiral Lagrangian (ECL) case [4]. For the sake of completeness, we have added the running of the ECLh parameters $a_4^r$ and $a_5^r$, which has been recently determined in the one-loop analysis of $WW$–scattering within the framework of chiral Lagrangians [7]. One can see that in the SM limit ($a = b = 1$) these $\mathcal{L}_4$ coefficients do not run, in agreement with the fact that these higher order operators are absent in the SM.

| | **ECLh** | **ECL** (Higgsless) |
|---|---|---|
| $\Gamma_{a_1-a_2+a_3}$ | $0$ | $0$ |
| $\Gamma_{c_\gamma}$ | $0$ | - |
| $\Gamma_{a_1}$ | $-\frac{1}{6}(1-a^2)$ | $-\frac{1}{6}$ |
| $\Gamma_{a_2-a_3}$ | $-\frac{1}{6}(1-a^2)$ | $-\frac{1}{6}$ |
| $\Gamma_{a_4}$ | $\frac{1}{6}(1-a^2)^2$ | $\frac{1}{6}$ |
| $\Gamma_{a_5}$ | $\frac{1}{8}(b-a^2)^2 + \frac{1}{12}(1-a^2)^2$ | $\frac{1}{12}$ |

where $e \sim \mathcal{O}(p/v)$ and $A$ and $B$ are given up to NLO by [5]

$$
\begin{aligned}
A(\gamma\gamma \to zz)_{\rm LO} &= B(\gamma\gamma \to zz)_{\rm LO} = 0\,, \\
A(\gamma\gamma \to zz)_{\rm NLO} &= \frac{2ac_\gamma^r}{v^2} + \frac{(a^2-1)}{4\pi^2 v^2}\,, \qquad B(\gamma\gamma \to zz)_{\rm NLO} = 0, \\
A(\gamma\gamma \to w^+w^-)_{\rm LO} &= 2sB(\gamma\gamma \to w^+w^-)_{\rm LO} = -\frac{1}{t} - \frac{1}{u}, \\
A(\gamma\gamma \to w^+w^-)_{\rm NLO} &= \frac{2ac_\gamma^r}{v^2} + \frac{(a^2-1)}{8\pi^2 v^2} + \frac{8(a_1^r - a_2^r + a_3^r)}{v^2}\,, \qquad B(\gamma\gamma \to w^+w^-)_{\rm NLO} = 0.
\end{aligned}
\tag{7}
$$

The term with $c_\gamma^r$ comes from the Higgs tree-level exchange in the $s$–channel, the term proportional to $(a^2-1)$ comes from the one-loop diagrams with $\mathcal{L}_2$ vertices, and the Higgsless operators in Eq. (5) yield the tree-level contribution to $\gamma\gamma \to w^+w^-$ proportional to $(a_1 - a_2 + a_3)$. Independent diagrams are in general UV divergent. However, in dimensional regularization, the final one-loop amplitude turns out to be UV finite and one has $a_1^r - a_2^r + a_3^r = a_1 - a_2 + a_3$, $c_\gamma^r = c_\gamma$ [5], as in the Higgsless case [19].

In order to pin down each of the relevant combinations of ECLh couplings in Eq. (7) ($a$, $c_\gamma^r$ and $a_1^r - a_2^r + a_3^r$) one must combine our $\gamma\gamma$-scattering analysis with other observables that depend on this same set of parameters. It is not difficult to find that other processes involving photons depend on these parameters. In Ref. [5] we computed 4 more observables of this kind: the $h \to \gamma\gamma$ decay width (depending on $a$ and $c_\gamma$), the oblique $S$–parameter (depending on $a$ and $a_1$), and the $\gamma^* \to w^+w^-$ (depending on $a$ and $a_2 - a_3$) and $\gamma^*\gamma \to h$ (depending on $c_\gamma$) electromagnetic form-factors. The one-loop contribution in these six relevant amplitudes is found to be UV-divergent in some cases. These divergences are absorbed by means of the generic $\mathcal{O}(p^4)$ renormalizations $a_i^r(\mu) = a_i + \delta a_i$. As expected, the renormalization in the six observables gives a fully consistent set of renormalization conditions and fixes the running of the renormalized couplings in the way given in Table 1.

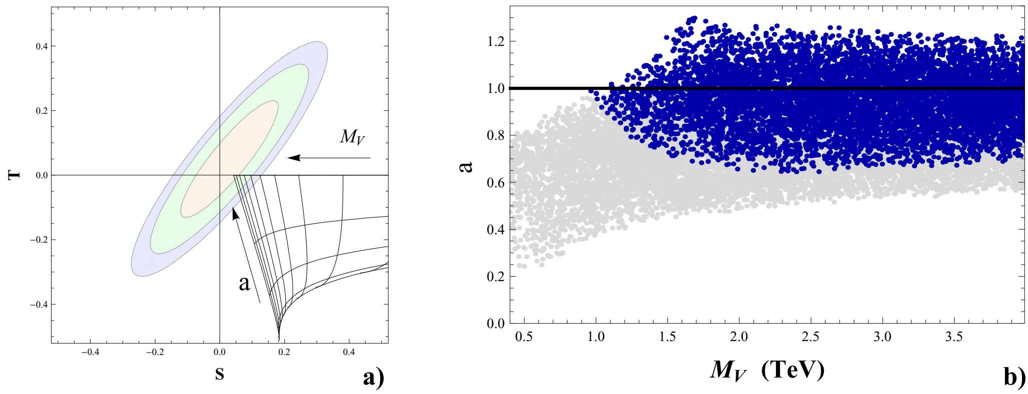


**Figure 1.** **a)** NLO determinations of $S$ and $T$, imposing the two WSRs. The approximately vertical curves correspond to constant values of $M_V$, from 1.5 to 6.0 TeV at intervals of 0.5 TeV. The approximately horizontal curves have constant values of $a$: $0.00, 0.25, 0.50, 0.75, 1.00$. The arrows indicate the directions of growing $M_V$ and $a$. The ellipses give the experimentally allowed regions at 68% (orange), 95% (green) and 99% (blue) confidence level (CL). **b)** Scatter plot for the 68% CL region, in the case when only the first WSR is assumed. The dark blue and light gray regions correspond, respectively, to $0.2 < M_V/M_A < 1$ and $0.02 < M_V/M_A < 0.2$.

## 3 Impact of spin–1 composite resonances on the oblique parameters

One can extend the range of validity and predictability of the ECLh by adding possible new states to the theory. Thus, the lightest V and A resonances are added to the EW Lagrangian in Ref. [14] in order to describe the oblique parameters $S$ and $T$ [9]. The relevant EW chiral invariant Lagrangian is given by the kinetic and Yang-Mills terms and the interactions [14] [2, 3]

$$\begin{aligned}\mathcal{L} &= \frac{v^2}{4}\langle u_\mu u^\mu\rangle\left(1+\frac{2\,a}{v}\,h\right)+\frac{F_V}{2\sqrt{2}}\langle V_{\mu\nu}f_+^{\mu\nu}\rangle+\frac{i\,G_V}{2\sqrt{2}}\langle V_{\mu\nu}[u^\mu,u^\nu]\rangle \\ &\quad+\frac{F_A}{2\sqrt{2}}\langle A_{\mu\nu}f_-^{\mu\nu}\rangle+\sqrt{2}\,\lambda_1^{hA}\,\partial_\mu h\,\langle A^{\mu\nu}u_\nu\rangle\,. \end{aligned}\tag{8}$$

In order to compute $S$ and $T$ up to the one-loop level we use the dispersive representations [9, 14],

$$S = \frac{16\pi}{g^2\tan\theta_W}\int_0^\infty\frac{\mathrm{d}t}{t}\,[\,\rho_S(t)-\rho_S(t)^{\mathrm{SM}}\,]\,,\qquad T=\frac{4\pi}{g'^2\cos^2\theta_W}\int_0^\infty\frac{\mathrm{d}t}{t^2}\,[\,\rho_T(t)-\rho_T(t)^{\mathrm{SM}}\,]\,,\tag{9}$$

with $\rho_S(t)$ the spectral function of the $W^3B$ correlator [9, 21] and $\rho_T(t)$ the spectral function of the difference of the neutral and charged Goldstone self-energies [14]. The calculation of $T$ above has been simplified by means of the Ward-Takahashi relation $T = Z^{(w^+)}/Z^{(w^0)} - 1$ [20]. Only the lightest two-particle cuts have been considered in $\rho_S(t)$ and $\rho_T(t)$, respectively, $\{ww, wh\}$ and $\{Bw, Bh\}$. Since $\rho_S(t)^{\mathrm{SM}} \stackrel{t\to\infty}{\longrightarrow} 0$, the convergence of the Peskin-Takeuchi sum-rule requires $\rho_S(t) \stackrel{t\to\infty}{\longrightarrow} 0$. Furthermore, assuming that weak isospin and parity are good symmetries of the BSM strong dynamics, the $W^3B$ correlator is proportional to the difference of the vector and axial-vector two-point Green's functions [9]. In asymptotically-free gauge theories this difference vanishes at $s\to\infty$ as $1/s^3$ [12], implying the (tree-level) LO WSRs [13],

$$F_V^2 - F_A^2 = v^2 \quad \text{(1st WSR)}, \qquad F_V^2\,M_V^2 - F_A^2\,M_A^2 = 0 \quad \text{(2nd WSR)}.\tag{10}$$

[2] Here we follow the notation $f_\pm^{\mu\nu} = u^\dagger\,\hat{W}^{\mu\nu}u \pm u\hat{B}^{\mu\nu}u^\dagger$ from Ref. [14, 21], where there is a global sign difference with [5] in the definitions of $\hat{W}_\mu$ and $\hat{B}_\mu$. The spin–1 resonances are described in the antisymmetric tensor formalism [8].

[3] In other works, the coupling $a$ can be found with the notation $\kappa_W$ and $\omega$ [14] or $\kappa_V$ [22].

**Table 2.** Allowed range for the $M_V$ and $a$ at the 68% CL for the two-WSRs (where $V$ and $A$ are very degenerate since $M_V^2/M_A^2 = a$ in this case) and only-1st-WSR cases (for various values $M_V/M_A$). In the last line we also impose the restriction† $M_V > 1$ TeV.

| | $a$ | $M_V$ |
|---|---|---|
| two WSRs | $0.97-1$ | $>5$ TeV |
| Only 1st WSR: $0.2 < M_V/M_A < 1$ | $0.6-1.3$ | $>1$ TeV |
| $0.5 < M_V/M_A < 1$ | $0.84-1.30$ | $>1.5$ TeV |
| $M_V/M_A = 1$ | $0.97-1.30$ | $>1.8$ TeV |
| $(M_V > 1\text{ TeV})^\dagger$ $1 < M_V/M_A < 2$ | $0.7-1.9$ | $>1$ TeV† |

However, although the 1st WSR is expected to be true in gauge theories with non-trivial ultraviolet fixed points [10, 11], the 2nd WSR is questionable in some of these models. Thus, two alternative scenarios are studied in Ref. [14]: one assuming the two WSRs and another assuming just the 1st WSR. At tree-level one has the the LO determinations [9, 14, 21]

$$S_{\mathrm{LO}} = 4\pi\left(\frac{F_V^2}{M_V^2} - \frac{F_A^2}{M_A^2}\right) = \frac{4\pi v^2}{M_V^2}\left(1+\frac{M_V^2}{M_A^2}\right) \qquad \text{(1st \& 2nd WSR)}, \tag{11}$$

$$S_{\mathrm{LO}} = 4\pi\left\{\frac{v^2}{M_V^2} + F_A^2\left(\frac{1}{M_V^2} - \frac{1}{M_A^2}\right)\right\} > \frac{4\pi v^2}{M_V^2} \qquad \text{(1st WSR \& } M_V < M_A).$$

In the first case, the two WSRs imply $M_V < M_A$ and determine $F_V$ and $F_A$ in terms of the resonance masses [8, 9, 14, 21]. In the second case, it is not possible to extract a definite prediction with just the 1st WSR but one can still derive the inequality above if one assumes a similar mass hierarchy $M_V < M_A$. On the other hand, this inequality flips direction if $M_A < M_V$ or turns into an equality in the degenerate case $M_V = M_A$ [14]. At NLO the computed $W^3B$ correlator is given by the $ww$ and $hw$ cuts, whose contributions to the $\rho_S(t)$ spectral function would have an unphysical grow at high energies unless $F_VG_V = v^2$ and $F_A\lambda_1^{hA} = av$ [8, 14, 21]. Thus, we obtain the NLO prediction [14]

$$\begin{aligned} S &= 4\pi v^2\left(\frac{1}{M_V^2} + \frac{1}{M_A^2}\right) \\ &\quad + \frac{1}{12\pi}\left[\log\frac{M_V^2}{m_H^2} - \frac{11}{6} + \frac{M_V^2}{M_A^2}\log\frac{M_A^2}{M_V^2} - \frac{M_V^4}{M_A^4}\left(\log\frac{M_A^2}{m_{S_1}^2} - \frac{11}{6}\right)\right] \qquad \text{(1st \& 2nd WSR)}, \\ S &> \frac{4\pi v^2}{M_V^2} + \frac{1}{12\pi}\left[\log\frac{M_V^2}{m_H^2} - \frac{11}{6} - a^2\left(\log\frac{M_A^2}{m_{S_1}^2} - \frac{17}{6} + \frac{M_A^2}{M_V^2}\right)\right], \qquad \text{(1st WSR \& } M_V < M_A). \end{aligned} \tag{12}$$

In the two-WSRs scenario, in order to enforce the 2nd WSR at NLO one needs the additional constraint $a = M_V^2/M_A^2$ (hence restricted to the range $0 \leq a \leq 1$). Again, the inequality in the last line flips direction or turns into an equality when, respectively, $M_A < M_V$ or $M_V = M_A$.

At LO, $\rho_T(t)$ is zero and one has $T_{\mathrm{LO}} = 0$. At NLO, where we enforce the $\rho_S(t)$ constraints $F_VG_V = v^2$ and $F_A\lambda_1^{hA} = av$, we find that $\rho_T(t) \xrightarrow{t\to\infty} 0$ and obtain the NLO prediction

$$T = \frac{3}{16\pi\cos^2\theta_W}\left[1 + \log\frac{m_h^2}{M_V^2} - a^2\left(1+\log\frac{m_h^2}{M_A^2}\right)\right], \tag{13}$$

In Fig. 1, we show the compatibility between the experimental determinations for $S$ and $T$ [15] and our NLO determinations in both scenarios. The numerical results in Table 2 show that the precision electroweak data requires resonance masses over the TeV and the $hWW$ coupling to be close to the SM one ($a^{\rm SM} = 1$), in agreement with present LHC bounds [22].

To conclude, we emphasize that, remarkably, just by considering the experimental $m_h$ (the only LHC input) and the EW precision observables (LEP input), the allowed region concentrates around $a \simeq 1$ for reasonable values of the splitting $M_V/M_A \sim \mathcal{O}(1)$ (see Fig. 1 and Table 2).

## References


[1] S. Weinberg, Physica A**96** (1979) 327; J. Gasser and H. Leutwyler, Annals Phys. **158** (1984) 142; Nucl. Phys. B **250** (1985) 465; Nucl. Phys. B **250** (1985) 517.

[2] T. Appelquist and C. W. Bernard, Phys. Rev. D **22** (1980) 200.

[3] A. C. Longhitano, Phys. Rev. D **22** (1980) 1166; Nucl. Phys. B **188** (1981) 118.

[4] Maria J. Herrero and Ester Ruiz Morales, Nucl.Phys. B**418** (1994) 431.

[5] R.L. Delgado, A. Dobado, M.J. Herrero, J.J. Sanz-Cillero, JHEP 1407 (2014) 149.

[6] J. Hirn and J. Stern, Phys.Rev. D**73** (2006) 056001; G. Buchalla and O. Catà, JHEP **1207** (2012) 101.

[7] D. Espriu and B. Yencho, Phys. Rev D **87** (2013) 055017; D. Espriu, F. Mescia and B. Yencho, Phys. Rev D **88** (2013) 055002; D. Espriu and B. Mescia, Phys.Rev. D**90** (2014) 015035; R. L. Delgado, A. Dobado, F. J. Llanes-Estrada, J.Phys. G**41** (2014) 025002; JHEP **1402** (2014) 121.

[8] G. Ecker *et al.*, Nucl. Phys. B **321** (1989) 311; G. Ecker *et al.*, Phys. Lett. B **223** (1989) 425.

[9] M. E. Peskin and T. Takeuchi, Phys. Rev. D **46** (1992) 381; Phys. Rev. Lett. **65** (1990) 964.

[10] A. Orgogozo and S. Rychkov, JHEP **1203** (2012) 046.

[11] T. Appelquist and F. Sannino, Phys. Rev. D **59** (1999) 067702.

[12] C. W. Bernard, A. Duncan, J. LoSecco and S. Weinberg, Phys. Rev. D **12** (1975) 792.

[13] S. Weinberg, Phys. Rev. Lett. **18** (1967) 507.

[14] A. Pich, I. Rosell and J.J. Sanz-Cillero, Phys.Rev.Lett. 110 (2013) 181801; JHEP 1401 (2014) 157.

[15] M. Baak *et al.*, Eur. Phys. J. C 72 (2012) 2205; http://gfitter.desy.de/; LEP Electroweak Working Group, http://lepewwg.web.cern.ch/LEPEWWG/.

[16] S. Matsuzaki *et al.*, Phys. Rev. D **75** (2007) 073002; R. Barbieri *et al.*, Phys. Rev. D **78** (2008) 036012; O. Catà and J.F. Kamenik, Phys. Rev. D **83** (2011) 053010; A. Orgogozo and S. Rychkov, JHEP **1306** (2013) 014.

[17] J. M. Cornwall, D. N. Levin and G. Tiktopoulos, Phys.Rev. D **10** (1974) 1145, Erratum-ibid. D **11** (1975) 972; C.E. Vayonakis, Lett.Nuovo Cim. **17** (1976) 383; B.W. Lee, C. Quigg and H.B. Thacker, Phys.Rev. D **16** (1977) 1519; G.J. Gounaris, R. Kogerler and H. Neufeld, Phys.Rev. D **34** (1986) 3257.

[18] M.B. Gavela, K. Kanshin, P.A.N. Machado and S. Saa, [arXiv:1409.1571 [hep-ph]].

[19] M. J. Herrero and E. Ruiz-Morales, Phys.Lett. B**296** (1992) 397; J. Bijnens and F. Cornet, Nucl. Phys. B **296** (1988) 557; J. F. Donoghue, B. R. Holstein and Y.C. Lin, Phys.Rev. D **37** (1988) 2423; J. Bijnens, S. Dawson and G. Valencia, Phys. Rev. D **44** (1991) 3555.

[20] R. Barbieri *et al.*, Nucl. Phys. B **409** (1993) 105.

[21] A. Pich, I. Rosell and J.J. Sanz-Cillero, JHEP 1208 (2012) 106.

[22] ATLAS Collaboration, Report No. ATLAS-CONF-2014-009; CMS Collaboration, Report No. CMS-PAS-HIG-14-009.